

STORM SURGES

R. A. Flather, Proudman Oceanographic Laboratory,
Bidston Hill, Prenton, UK

Copyright © 2001 Academic Press

doi:10.1006/rwos.2001.0124

Introduction and Definitions

Storm surges are changes in water level generated by atmospheric forcing; specifically by the drag of the wind on the sea surface and by variations in the surface atmospheric pressure associated with storms. They last for periods ranging from a few hours to 2 or 3 days and have large spatial scales compared with the water depth. They can raise or lower the water level in extreme cases by several meters; a raising of level being referred to as a 'positive' surge, and a lowering as a 'negative' surge. Storm surges are superimposed on the normal astronomical tides generated by variations in the gravitational attraction of the moon and sun. The storm surge component can be derived from a time-series of sea levels recorded by a tide gauge using:

$$\begin{aligned} \text{surge residual} = & (\text{observed sea level}) \\ & - (\text{predicted tide level}) \end{aligned} \quad [1]$$

producing a time-series of surge elevations. Figure 1 shows an example.

Sometimes, the term 'storm surge' is used for the sea level (including the tidal component) during a storm event. It is important to be clear about the usage of the term and its significance to avoid confusion. Storms also generate surface wind waves that have periods of order seconds and wavelengths, away from the coast, comparable with or less than the water depth.

Positive storm surges combined with high tides and wind waves can cause coastal floods, which, in terms of the loss of life and damage, are probably the most destructive natural hazards of geophysical origin. Where the tidal range is large, the timing of the surge relative to high water is critical and a large surge at low tide may go unnoticed. Negative surges reduce water depth and can be a threat to navigation. Associated storm surge currents, superimposed on tidal and wave-generated flows, can also contribute to extremes of current and bed stress responsible for coastal erosion. A proper understanding of storm surges, the ability to predict them and measures to mitigate their destructive effects are therefore of vital concern.

Storm Surge Equations

Most storm surge theory and modeling is based on depth-averaged hydrodynamic equations applicable to both tides and storm surges and including nonlinear terms responsible for their interaction. In vector form, these can be written:

$$\frac{\partial \zeta}{\partial t} + \nabla \cdot (D\mathbf{q}) = 0 \quad [2]$$

$$\begin{aligned} \frac{\partial \mathbf{q}}{\partial t} + \mathbf{q} \cdot \nabla \mathbf{q} - f\mathbf{k} \times \mathbf{q} = & -g\nabla(\zeta - \bar{\zeta}) - \frac{1}{\rho} \nabla p_a \\ & + \frac{1}{\rho D} (\boldsymbol{\tau}_s - \boldsymbol{\tau}_b) + A\nabla^2 \mathbf{q} \end{aligned} \quad [3]$$

where t is time; ζ the sea surface elevation; $\bar{\zeta}$ the equilibrium tide; \mathbf{q} the depth-mean current; $\boldsymbol{\tau}_s$ the wind stress on the sea surface; $\boldsymbol{\tau}_b$ the bottom stress; p_a atmospheric pressure on the sea surface; D the total water depth ($D = h + \zeta$, where h is the undisturbed depth); ρ the density of sea water, assumed to be uniform; g the acceleration due to gravity; f the Coriolis parameter ($= 2\omega \sin\phi$, where ω is the angular speed of rotation of the Earth and ϕ is the latitude); \mathbf{k} a unit vector in the vertical; and A the coefficient of horizontal viscosity. Eqn [2] is the continuity equation expressing conservation of volume. Eqn [3] equates the accelerations (left-hand side) to the force per unit mass (right-hand side).

In this formulation, bottom stress, $\boldsymbol{\tau}_b$ is related to the current, \mathbf{q} , using a quadratic law:

$$\boldsymbol{\tau}_b = k\rho\mathbf{q}|\mathbf{q}| \quad [4]$$

where k is a friction parameter (~ 0.002). Similarly, the wind stress, $\boldsymbol{\tau}_s$, is related to \mathbf{W} , the wind velocity at a height of 10 m above the surface, also using a quadratic law:

$$\boldsymbol{\tau}_s = c_D \rho_a \mathbf{W}|\mathbf{W}| \quad [5]$$

where ρ_a is the density of air and c_D a drag coefficient. Measurements in the atmospheric boundary layer suggest that c_D increases with wind speed, W , accounting for changes in surface roughness associated with wind waves. A typical form due to J. Wu is:

$$10^3 c_D = 0.8 + 0.065W \quad [6]$$

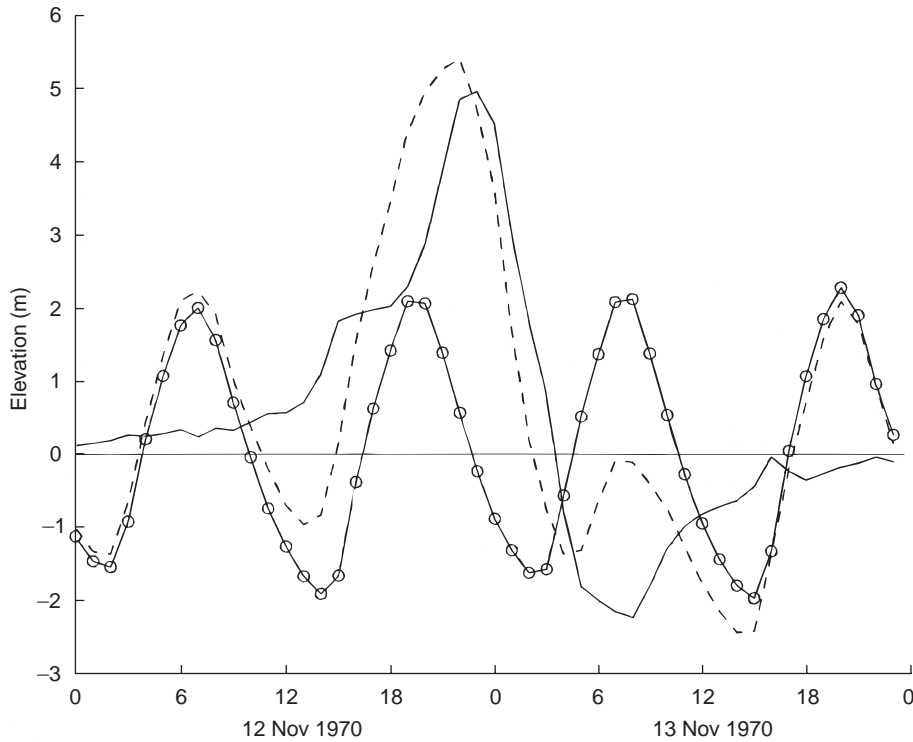


Figure 1 Water level (dashed line), predicted tide (line with ○), and the surge residual (continuous line) at Sandwip Island, Bangladesh, during the catastrophic storm surge of 12–13 November 1970 (times are GMT).

Alternatively, from dimensional analysis, H. Charnock obtained $gz_0/u_*^2 = \alpha$, where z_0 is the aerodynamic roughness length associated with the surface wavefield, u_* is the friction velocity ($u_*^2 = \tau_s/\rho_a$), and α is the Charnock constant. So, the roughness varies linearly with surface wind stress. Assuming a logarithmic variation of wind speed with height z above the surface, $W(z) = (u_*/\kappa) \ln(z/z_0)$, where κ is von Kármán's constant. It follows that for $z = 10\text{ m}$:

$$c_D = [(1/\kappa)\ln\{gz/(\alpha c_D W^2)\}]^{-2} \quad [7]$$

Estimates of α range from 0.012 to 0.035.

Generation and Dynamics of Storm Surges

The forcing terms in eqn [3] which give rise to storm surges are those representing wind stress and the horizontal gradient of surface atmospheric pressure. Very simple solutions describe the basic mechanisms. The sea responds to atmospheric pressure variations by adjusting sea level such that, at depth, pressure in the water is uniform, the hydrostatic approximation. Assuming in eqn [3] that $\mathbf{q} = 0$ and

$\tau_s = 0$, then $g\nabla\zeta + (1/\rho)\nabla p_a = 0$, so $\rho g\zeta + p_a = \text{constant}$. This gives the 'inverse barometer effect' whereby a decrease in atmospheric pressure of 1 hPa produces an increase in sea level of approximately 1 cm. Wind stress produces water level variations on the scale of the storm. Eqns [5] and [6] imply that the strongest winds are most important since effectively $\tau_s \propto W^3$. Both pressure and wind effects are present in all storm surges, but their relative importance varies with location. Since wind stress is divided by D whereas ∇p_a is not, it follows that wind forcing increases in importance in shallower water. Consequently, pressure forcing dominates in the deep ocean whereas wind forcing dominates in shallow coastal seas. Major destructive storm surges occur when extreme storm winds act over extensive areas of shallow water.

As well as the obvious wind set-up, with the component of wind stress directed towards the coast balanced by a surface elevation gradient, winds parallel to shore can also generate surges at higher latitudes. Wind stress parallel to the coast with the coast on its right will drive a longshore current, limited by bottom friction. Geostrophic balance gives (in the Northern Hemisphere) a surface gradient raising levels at the coast (*see Tides*).

Amplification of surges may be caused by the funneling effect of a converging coastline or estuary and by a resonant response; e.g. if the wind forcing travels at the same velocity as the storm wave, or matches the natural period of oscillation of a gulf, producing a seiche.

As a storm moves away, surges generated in one area may propagate as free waves, contributing as externally generated components to surges in another area. Generally, away from the forcing center, the response of the ocean consists of longshore propagating coastally trapped waves. Examples include external surges in the North Sea (see **Figure 2**), which are generated west and north of Scotland and propagate anticlockwise round the basin like the diurnal tide; approximately as a Kelvin wave. Low mode continental shelf waves have been identified in surges on the west coast of Norway, in the Middle Atlantic Bight of the US, in the East China Sea, and on the north-west shelf of Australia. Currents associated with low mode continental shelf waves generated by a tropical cyclone crossing the north-west shelf of Australia have been observed and explained by numerical modeling. Edge waves can also be generated by cyclones travelling parallel to the coast in the opposite direction to shelf waves.

From eqns [3] and [4], bottom stress (which dissipates surges) also depends on water depth and is non-linear; the current including contributions from tide and surge, $\mathbf{q} = \mathbf{q}_T + \mathbf{q}_S$. Consequently, dissipation of surges is stronger in shallow water and where tidal currents are also strong. In deeper water and where tides are weak, free motions can persist for long times or propagate long distances. For example, the Adriatic has relatively small tides and seiches excited by storms can persist for many days.

In areas with substantial tides and shallow water, non-linear dynamical processes are important, resulting in interactions between the tide and storm surge such that both components are modified. The main contribution arises from bottom stress, but time-dependent water depth, $D = h + \zeta(t)$, can also be significant (e.g. $\tau_s/(\rho D)$ will be smaller at high tide than at low tide). An important consequence is that the linear superposition of surge and tide without accounting for their interaction gives substantial errors in estimating water level. For example, for surges propagating southwards in the North Sea into the Thames Estuary, surge maxima tend to occur on the rising tide rather than at high water (**Figure 3**).

Interactions also occur between the tide–surge motion and surface wind waves (see below).

Areas Affected by Storm Surges

Major storm surges are created by mid-latitude storms and by tropical cyclones (also called hurricanes and typhoons) which generally occur in geographically separated areas and differ in their scale. Mid-latitude storms are relatively large and evolve slowly enough to allow accurate predictions of their wind and pressure fields from atmospheric forecast models. In tropical cyclones, the strongest winds occur within a few tens of kilometers of the storm center and so are poorly resolved by routine weather prediction models. Their evolution is also rapid and much more difficult to predict. Consequently prediction and mitigation of the effects of storm surges is further advanced for mid-latitude storms than for tropical cyclones.

Tropical cyclones derive energy from the warm surface waters of the ocean and develop only where the sea surface temperature (SST) exceeds 26.5°C. Since their generation is dependent on the effect of the local vertical component of the Earth's rotation, they do not develop within 5° of the equator. **Figure 4** shows the main cyclone tracks. Areas affected include: the continental shelf surrounding the Gulf of Mexico and on the east coast of the US (by hurricanes); much of east Asia including Vietnam, China, the Philippines and Japan (by typhoons); the Bay of Bengal, in particular its shallow north-east corner, and northern coasts of Australia (by tropical cyclones). Areas affected by mid-latitude storms include the North Sea, the Adriatic, and the Patagonian Shelf. Inland seas and large lakes, including the Great Lakes, Lake Okechobee (Florida), and Lake Biwa (Japan) also experience surges.

The greatest loss of life due to storm surges has occurred in the northern Bay of Bengal and Meghna Estuary of Bangladesh. A wide and shallow continental shelf bounded by extensive areas of low-lying poorly protected land is impacted by tropical cyclones. Cyclone-generated storm surges on 12–13 November 1970 and 29–30 April 1991 (**Figure 5**) killed approximately 250 000 and 140 000 people, respectively, in Bangladesh.

A severe storm in the North Sea on 31 January–1 February 1953 generated a large storm surge, which coincided with a spring tide to cause catastrophic floods in the Netherlands (**Figure 6**) and south-east England, killing approximately 2000 people. Subsequent government enquiries resulted in the 'Delta Plan' to improve coastal defences in Holland, led to the setting up of coastal flood warning authorities, and accelerated research into storm surge dynamics.

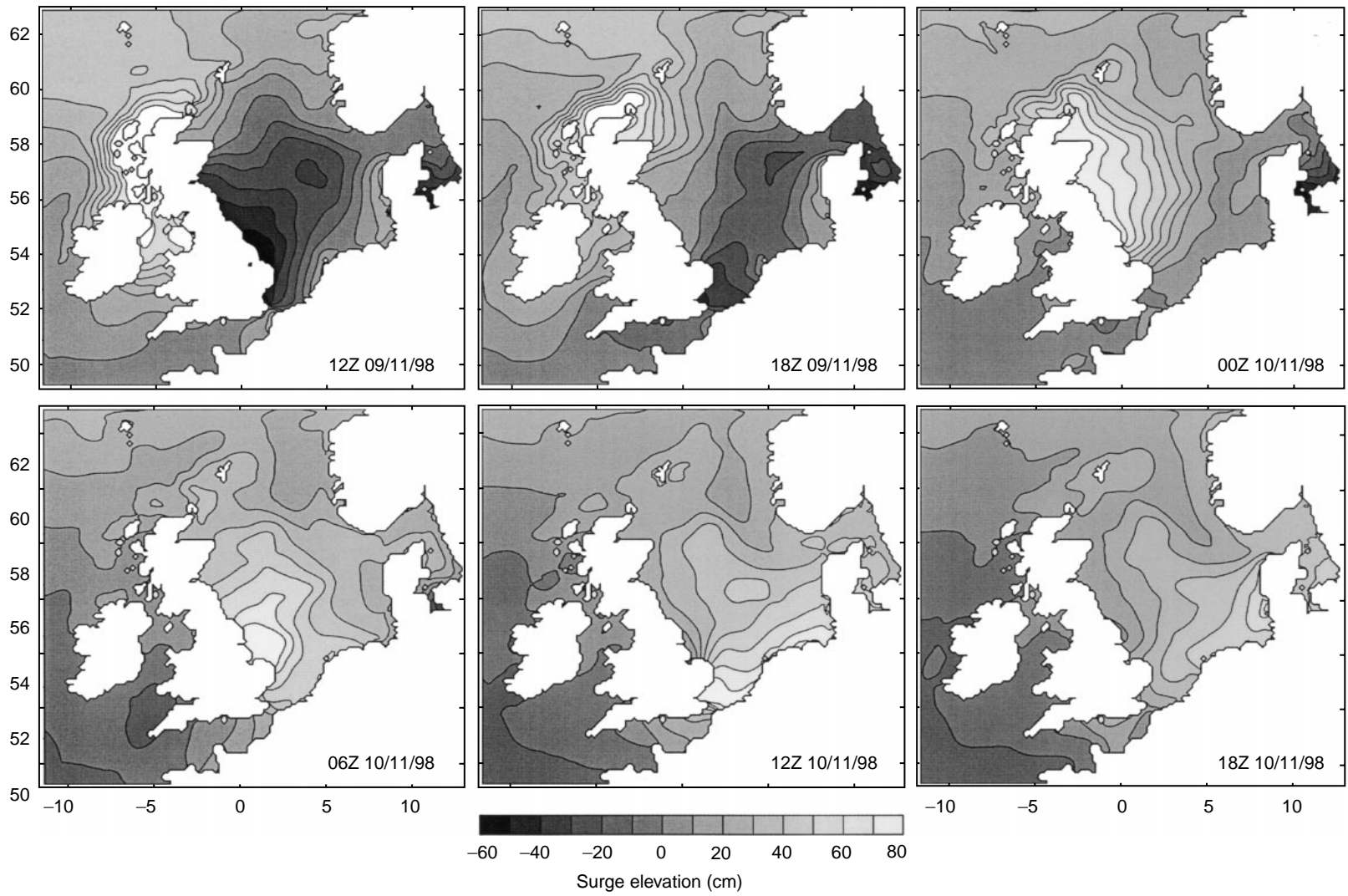


Figure 2 Propagation of an external surge in the North Sea from a numerical model simulation.

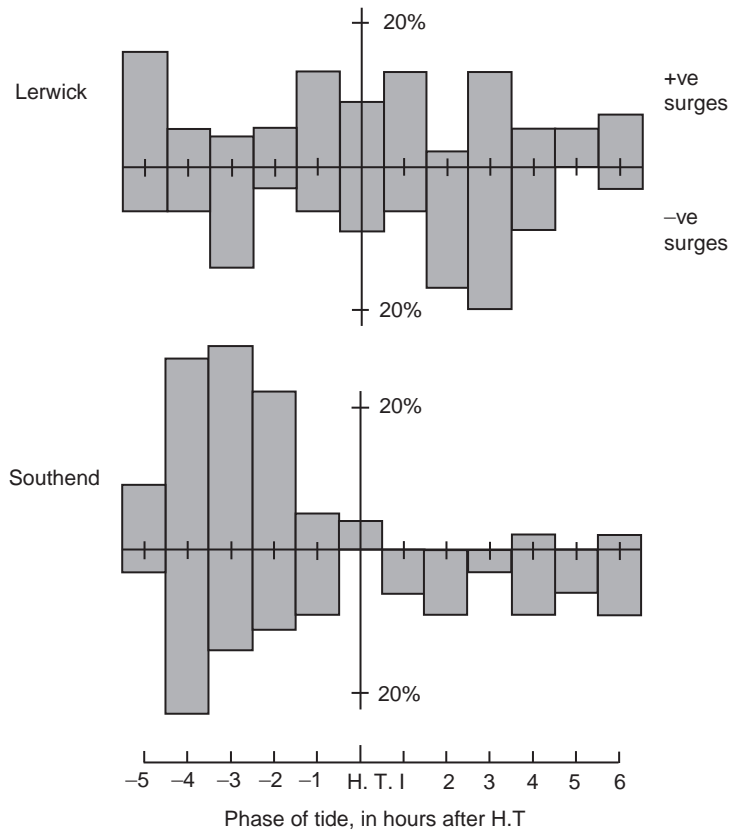


Figure 3 Frequency distribution relative to the time of tidal high water of positive and negative surges at Lerwick (northern North Sea) and Southend (Thames Estuary). The phase distribution at Lerwick is random, whereas due to tide–surge interaction most surge peaks at Southend occur on the rising tide (re-plotted from Prandle D and Wolf J, 1978, *The interaction of surge and tide in the North Sea and River Thames. Geophys. J. R. Astr. Soc.*, 55: 203–216, by permission of the Royal Astronomical Society).

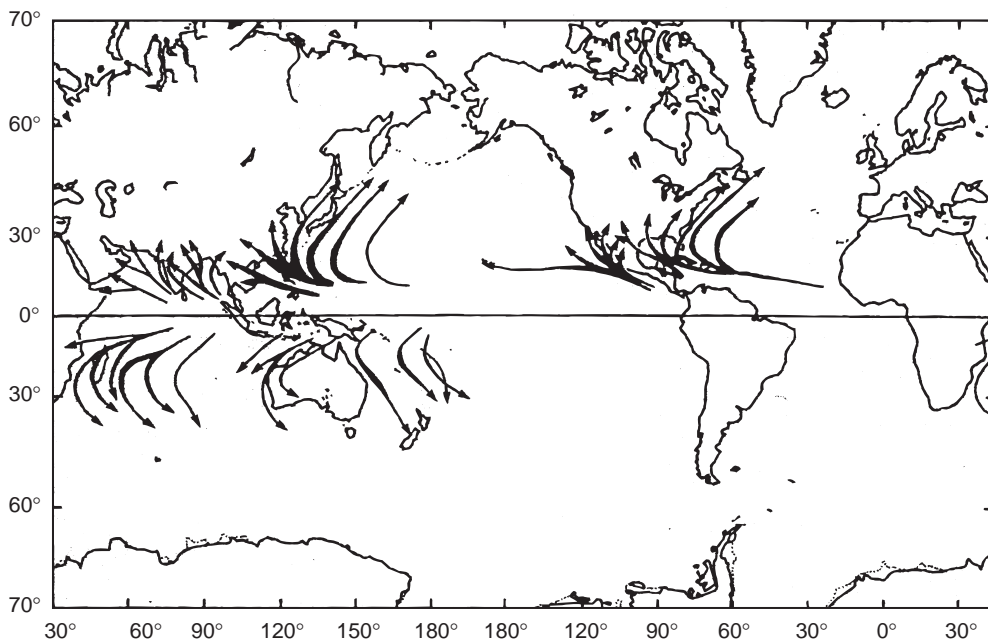


Figure 4 Tropical cyclone tracks (from Murty, 1984, reproduced by permission of the Department of Fisheries and Oceans, Canada).

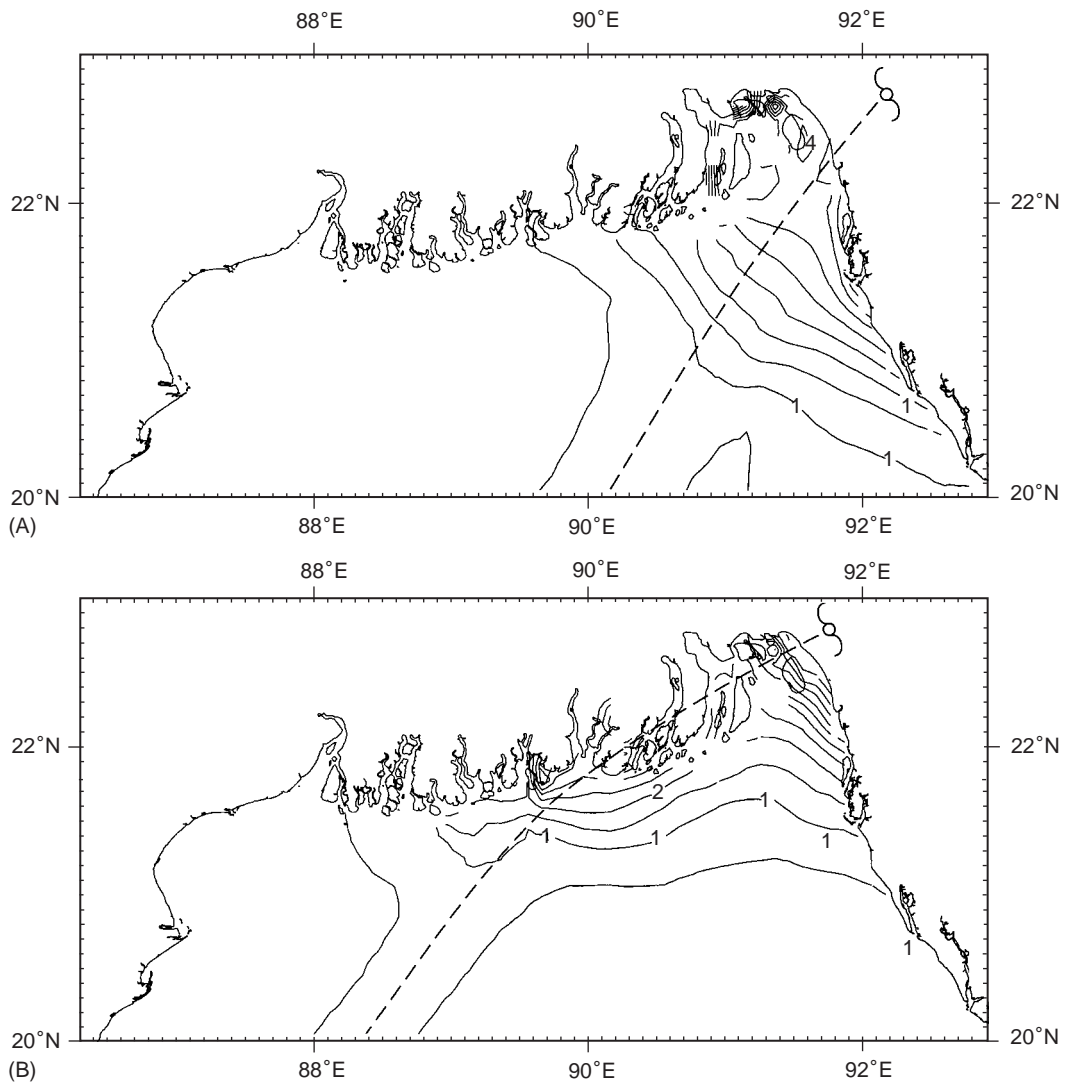


Figure 5 Cyclone tracks (dashed lines) and maximum computed surge elevation measured in meters in the northern Bay of Bengal during the cyclones of (A) 1970 and (B) 1991 from numerical model simulations (contour interval 0.5 m). (Re-plotted from Flather, 1994, by permission of the American Meteorological Society.)

The city of Venice, in Italy, suffers frequent ‘acqua alta’ which flood the city, disrupting its life and accelerating the disintegration of the unique historic buildings.

In 1969 Hurricane Camille created a surge in the Gulf of Mexico which rose to 7 m above mean sea level, causing more than 100 deaths and about 1 billion dollars worth of damage. An earlier cyclone in the region, in 1900, flooded the island of Galveston, Texas, with the loss of 6000 lives.

Storm Surge Prediction

Early research on storm surges was based on analysis of observations and solution of simplified – usually linearized – equations for surges in idealized

channels, rectangular gulfs, and basins with uniform depth. The first self-recording tide gauge was installed in 1832 at Sheerness in the Thames Estuary, England, so datasets for analysis were available from an early stage. Interest was stimulated by events such as the 1953 storm surge in the North Sea, which highlighted the need for forecasts.

First prediction methods were based on empirical formulae derived by correlating storm surge elevation with atmospheric pressure, wind speed and direction and, where appropriate, observed storm surges from a location ‘upstream’. Long time-series of observations are required to establish reliable correlations. Where such observations existed, e.g. in the North Sea, the methods were quite successful.



Figure 6 Breached dyke in the Netherlands after the 1953 North Sea storm surge. (Reproduced by permission of RIKZ, Ministry of Public Works, The Netherlands.)

From the 1960s, developments in computing and numerical techniques made it possible to simulate and predict storm surges by solving discrete approximations to the governing equations (eqns [1] and [2]). The earliest and simplest methods, pioneered in Europe by W. Hansen and N.S. Heaps and in the USA by R.O. Reid and C.P. Jelesnianski, used a time-stepping approach based on finite difference approximations on a regular grid. Surge-tide interaction could be accounted for by solving the non-linear equations and including tide. Effects of inundation could also be included by allowing for moving boundaries; water levels computed with a fixed coast can be $O(10\%)$ higher than those with flooding of the land allowed.

Recent developments have revolutionized surge modeling and prediction. Among these, coordinate transformations, curvilinear coordinates and grid nesting allow better fitting of coastal boundaries and enhanced resolution in critical areas. A simple example is the use of polar coordinates in the SLOSH (Sea, Lake and Overland Surges from Hurricanes) model focusing on vulnerable sections of the US east coast. Finite element methods with even greater flexibility in resolution (e.g. **Figure 7**) have also been used in surge computations in recent years.

There has also been increasing use of three-dimensional (3-D) models in storm surge studies. Their main advantage is that they provide information on the vertical structure of currents and, in particular, allow the bottom stress to be related to flow near the seabed. This means that in a 3-D formulation the bottom stress need not oppose the direction of the depth mean flow and hence of the

water transport. Higher surge estimates result in some cases.

In the last decades many countries have established and now operate model-based flood warning systems. Although finite element methods and 3-D models have been developed and are used extensively for research, most operational models are still based on depth-averaged finite-difference formulations.

A key requirement for accurate surge forecasts is accurate specification of the surface wind stress. Surface wind and pressure fields from numerical weather prediction (NWP) models are generally used for mid-latitude storms. Even here, resolution of small atmospheric features can be important, so preferably NWP data at a resolution comparable with that of the surge model should be used. For tropical cyclones, the position of maximum winds at landfall is critical, but prediction of track and evolution (change in intensity, etc.) is problematic. Presently, simple models are often used based on basic parameters: p_c , the central pressure; W_m , the maximum sustained 10 m wind speed; R , the radius to maximum winds; and the velocity, V , of movement of the cyclone's eye. Assuming a pressure profile, e.g. that due to G.J. Holland:

$$p_a(r) = p_c + \Delta p \exp[-(R/r)^B] \quad [8]$$

where r is the radial distance from the cyclone center, Δp the pressure deficit (difference between the ambient and central pressures), and B is a 'peakedness' factor typically $1.0 < B < 2.5$. Wind fields can then be estimated using further assumptions and approximations. First, the gradient or

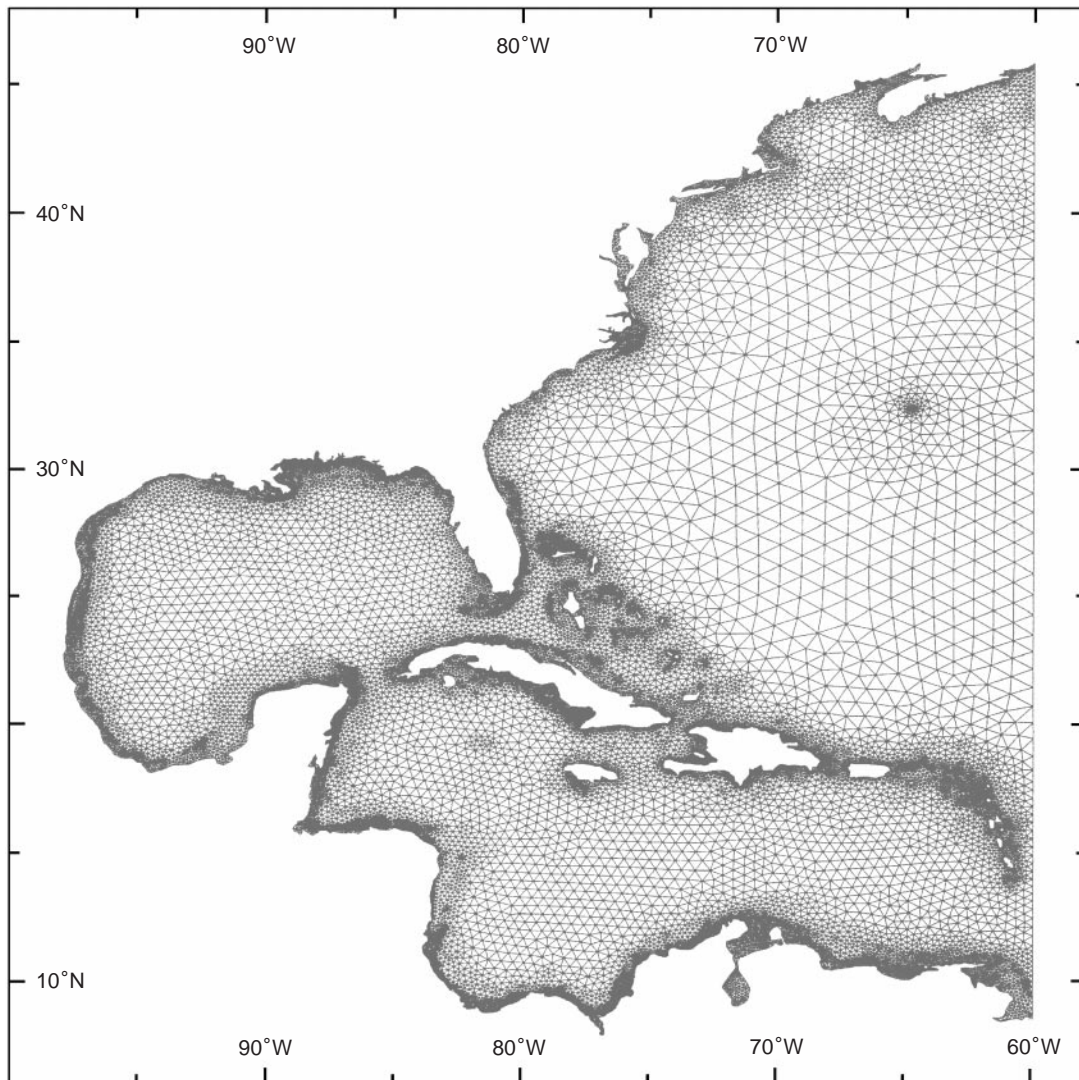


Figure 7 A finite element grid for storm surge calculations on the east coast of the USA, the Gulf of Mexico, and Caribbean (from Blain CA, Westerink JJ and Leutlich RL (1994) The influence of domain size on the response characteristics of a hurricane storm surge model. *J. Geophys. Res.*, 99(C9) 18467–18479. Reproduced by permission of the American Geophysical Union.)

cyclostrophic wind can be calculated as a function of r . An empirical factor (~ 0.8) reduces this to W , the 10 m wind. A contribution from the motion of the storm (maybe 50% of V) can be added, introducing asymmetry to the wind field, and finally to account for frictional effects in the atmospheric boundary layer, wind vectors may be turned inwards by a cross-isobar angle of 10° – 25° . Such procedures are rather crude, so that cyclone surges computed using the resulting winds are unlikely to be very accurate. Simple vertically integrated models of the atmospheric boundary layer have been used to compute winds from a pressure distribution such as eqn [8], providing a more consistent approach. In reality, cyclones interact with the ocean. They

generate wind waves, which modify the sea surface roughness, z_0 , and hence the wind stress generating the surge. Wind- and wave-generated turbulence mixes the surface water changing its temperature and so modifies the flux of heat from which the cyclone derives its energy. Progress requires improved understanding of air–sea exchanges at extreme wind speeds and high resolution coupled atmosphere–ocean models.

Interactions with Wind Waves

As mentioned above, observations suggested that Charnock's α was not constant but depended on water depth and 'wave age', a measure of the state

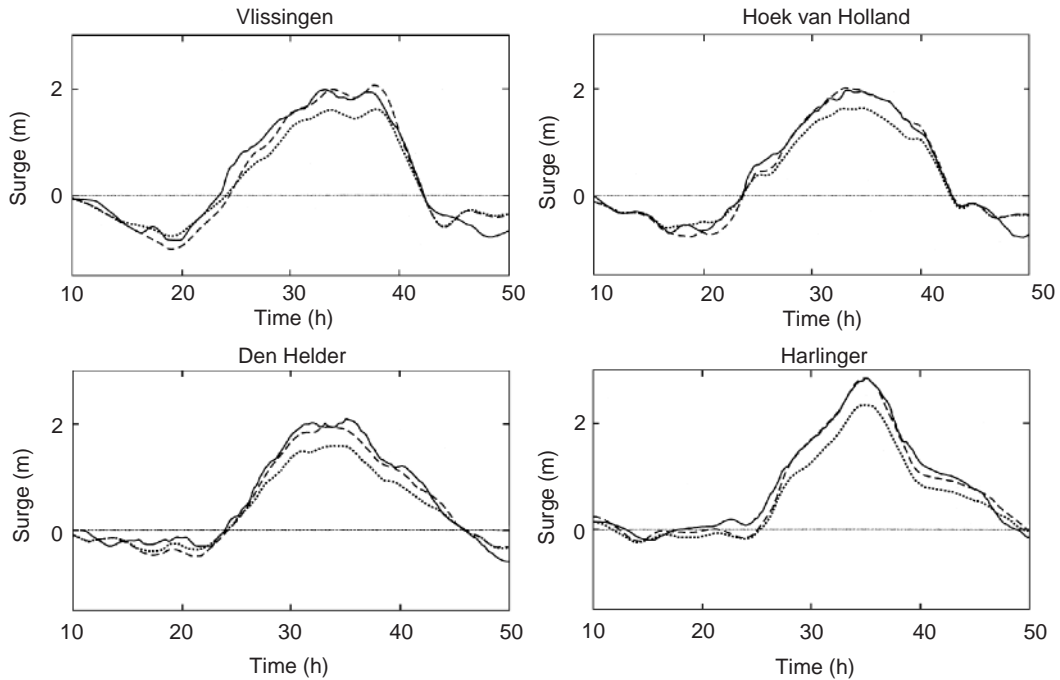


Figure 8 Computed surge elevations during 13–16 February 1989 with (dashed line) and without (dotted) wave stress compared with observations (continuous line). (Re-plotted from Mastenbroek *et al.*, 1994 by permission of the American Geophysical Union.)

of development of waves. Young waves are steeper and propagate more slowly, relative to the wind speed, than fully developed waves and so are aerodynamically rougher enhancing the surface stress. These effects can be incorporated in a drag coefficient which is a function of wave age, wave height, and water depth and agrees well with published datasets over the whole range of wave ages. Further research, considering the effects of waves on airflow in the atmospheric boundary layer, led P.A.E.M. Janssen to propose a wave-induced stress enhancing the effective roughness. Application of this theory requires the dynamical coupling of surge and wave models such that friction velocity and roughness determine and are determined by the waves. Mastenbroek *et al.* obtained improved agreement with observed surges on the Dutch coast by including the wave-induced stress in a model experiment (Figure 8). However, they also found that the same improvement could be obtained by a small increase in the standard drag coefficient.

In shallow water, wave orbital velocities also reach the seabed. The bottom stress acting on surge and tide is therefore affected by turbulence introduced at the seabed in the wave boundary layer. With simplifying assumptions, models describing these effects have been developed and can be used in storm surge modeling. Experiments using both 2-D and 3-D surge models have been carried out. 3-D

modeling of surges in the Irish Sea using representative waves shows significant effects on surge peaks and improved agreement with observations. Bed stresses are much enhanced in shallow water. Because the processes depend on the nature of the bed, a more complete treatment should take account of details of bed types.

Non-linear interactions give rise to a wave-induced mean flow and a change in mean water depth (wave set-up and set-down). The former has contributions from a mean momentum density produced by a non-zero mean flow in the surface layer (above the trough level of the waves), and from wave breaking. Set-up and set-down arise from the ‘radiation stress’, which is defined as the excess momentum flux due to the waves (*see Waves on Beaches*). Mastenbroek *et al.* showed that the radiation stress has a relatively small influence on the calculated water levels in the North Sea but cannot be neglected in all cases. It is important where depth-induced changes in the waves, as shoaling or breaking, dominate over propagation and generation, i.e. in coastal areas. The effects should be included in the momentum equations of the surge model.

Although ultimately coupled models with a consistent treatment of exchanges between atmosphere and ocean and at the seabed remain a goal, it appears that with the present state of understanding the benefits may be small compared with other

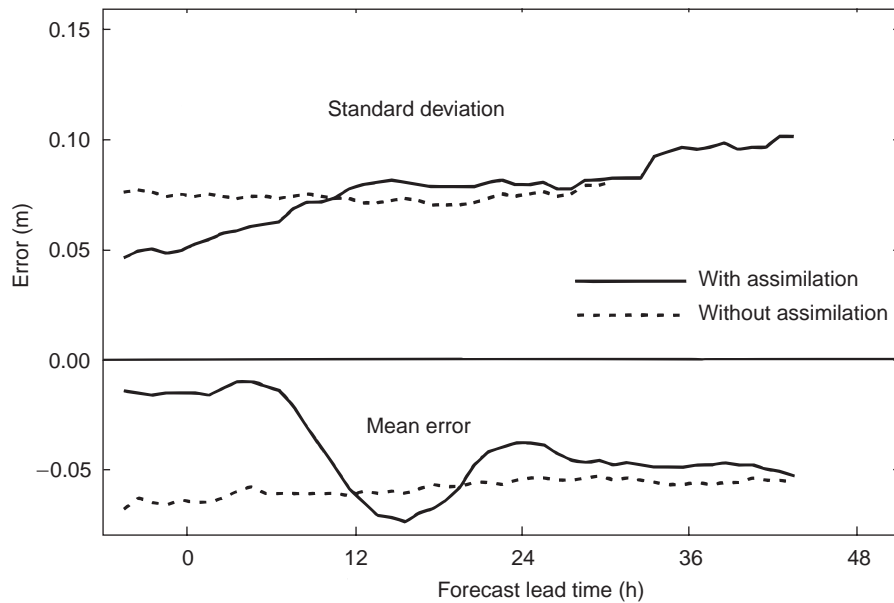


Figure 9 Variation of forecast errors in surge elevation with forecast lead-time from the Dutch operational model with (continuous line) and without (dashed line) assimilation of tide gauge data. (Replotted from Flather, 2000, by permission of Elsevier Science BV.)

inherent uncertainties. In particular, accurate definition of the wind field itself and details of bed types (rippled or smooth, etc.) are not readily available.

Data Assimilation

Data assimilation plays an increasing role, making optimum use of real-time observations to improve the accuracy of initial data in forecast models. Bode and Hardy (see Further Reading section) reviewed two approaches, involving solution of adjoint equations and Kalman filtering. The Dutch operational system has used Kalman filtering since 1992, incorporating real-time tide gauge data from the east coast of Britain. Accuracy of predictions (Figure 9) is improved for the first 10–12 h of the forecast.

Related Issues

Extremes

Statistical analysis of storm surges to derive estimates of extremes is important for the design of coastal defenses and safety of offshore structures. This requires long time-series of surge elevation derived from observations of sea level where available or, increasingly, from model hindcasts covering O(50 years) forced by meteorological analyses.

Climate Change Effects

Climate change will result in a rise in sea level and possible changes in storm tracks, storm intensity

and frequency, collectively referred to as ‘storminess’. Changes in water depth with rising mean sea level (MSL) will modify the dynamics of tides and surges, increasing wavelengths and modifying the generation, propagation, and dissipation of storm surges. Increased water depth implies a small reduction in the effective wind stress forcing, suggesting smaller surges. However, effects of increased storminess may offset this. It has been suggested, for example, that increased temperatures in some regions could raise sea surface temperatures resulting in more intense and more frequent tropical cyclones. Regions susceptible to tropical cyclones could also be extended. Research is in progress to assess and quantify some of these effects, e.g. with tide–surge models forced by outputs from climate GCMs. An important issue is that of distinguishing climate-induced change from the natural inter-annual and decadal variability in storminess and hence surge extremes.

See also

Fish Feeding and Foraging. Tides. Waves on Beaches. Wind Driven Circulation.

Further Reading

Bode L and Hardy TA (1997) Progress and recent developments in storm surge modelling. *Journal of Hydraulic Engineering* 123(4): 315–331.

- Flather RA (1994) A storm surge prediction model for the northern Bay of Bengal with application to the cyclone disaster in April 1991. *Journal of Physical Oceanography* 24: 172–190.
- Flather RA (2000) Existing operational oceanography. *Coastal Engineering* 41: 13–40.
- Heaps NS (1967) Storm surges. In: Bavnés H (ed.) *Oceanography and Marine Biology Annual Review* 5: 11–47. London, Allen and Unwin.
- Mastenbroek C, Burgers G and Janssen PAEM (1993) The dynamical coupling of a wave model and a storm surge model through the atmospheric boundary layer. *Journal of Physical Oceanography* 23: 1856–1866.
- Murty TS (1984) Storm surges – meteorological ocean tides. *Canadian Bulletin of Fisheries and Aquatic Sciences* 212: 1–897.
- Murty TS, Flather RA and Henry RF (1986) The storm surge problem in the Bay of Bengal. *Progress in Oceanography* 16: 195–233.
- Pugh DT (1987) *Tides, Surges, and Mean Sea Level*. Chichester: John Wiley & Sons.
- World Meteorological Organisation (1978) *Present Techniques of Tropical Storm Surge Prediction*. Report 13. Marine science affairs, WMO No. 500. Geneva, Switzerland.

SUB ICE-SHELF CIRCULATION AND PROCESSES

K. W. Nicholls, British Antarctic Survey, Cambridge, UK

Copyright © 2001 Academic Press

doi:10.1006/rwos.2001.0010

Introduction

Ice shelves are the floating extension of ice sheets (*see Ice-shelf Stability*). They extend from the grounding line, where the ice sheet first goes afloat, to the ice front, which usually takes the form of an ice cliff dropping down to the sea. Although there are several examples on the north coast of Greenland, the largest ice shelves are found in the Antarctic where they cover 40% of the continental shelf. Ice shelves can be up to 2 km thick and have horizontal extents of several hundreds of kilometers. The base of an ice shelf provides an intimate link between ocean and cryosphere. Three factors control the oceanographic regime beneath ice shelves: the geometry of the sub-ice shelf cavity, the oceanographic conditions beyond the ice front, and tidal activity. These factors combine with the thermodynamics of the interaction between sea water and the ice shelf base to yield various glaciological and oceanographic phenomena: intense basal melting near deep grounding lines and near ice fronts; deposition of ice crystals at the base of some ice shelves, resulting in the accretion of hundreds of meters of marine ice; production of sea water at temperatures below the surface freezing point, which may then contribute to the formation of Antarctic Bottom Water (*see Bottom Water Formation*); and the upwelling of relatively warm Circumpolar Deep Water.

Although the presence of the ice shelf itself makes measurement of the sub-ice shelf environment

difficult, various field techniques have been used to study the processes and circulation within sub-ice shelf cavities. Rates of basal melting and freezing affect the flow of the ice and the nature of the ice–ocean interface, and so glaciological measurements can be used to infer the ice shelf's basal mass balance. Another indirect approach is to make ship-based oceanographic measurements along ice fronts. The properties of in-flowing and out-flowing water masses give clues as to the processes needed to transform the water masses. Direct measurements of oceanographic conditions beneath ice shelves have been made through natural access holes such as rifts, and via access holes created using thermal (mainly hot-water) drills. Numerical models of the sub-ice shelf regime have been developed to complement the field measurements. These range from simple one-dimensional models following a plume of water from the grounding line along the ice shelf base, to full three-dimensional models coupled with sea ice models, extending out to the continental shelf-break and beyond.

The close relationship between the geometry of the sub-ice shelf cavity and the interaction between the ice shelf and the ocean implies a strong dependence of the ice shelf/ocean system on the state of the ice sheet. During glacial climatic periods the geometry of ice shelves would have been radically different to their geometry today, and ice shelves probably played a different role in the climate system.

Geographical Setting

By far the majority of the world's ice shelves are found fringing the Antarctic coastline (**Figure 1**). Horizontal extents vary from a few tens to several hundreds of kilometers, and maximum thickness at